

The optical detection of individual DNA-conjugated gold nanoparticle labels after metal enhancement

Andrea Csáki, Pia Kaplanek, Robert Möller and Wolfgang Fritzsche

Institute for Physical High Technology, PF 100239, D-07702 Jena, Germany

Received 30 June 2003, in final form 13 October 2003

Published 22 October 2003

Online at stacks.iop.org/Nano/14/1262

Abstract

The detection of DNA using nanoparticles as labels is an interesting alternative to the standard fluorescence technique. It requires simpler detection equipment, resulting in higher stability and lower costs. Besides easier detection, metal enhancement allows a higher sensitivity of detection. The signal-response curve for labelled DNA before and after silver enhancement was studied, applying both atomic force microscope (AFM) and optical (reflection/transmission) measurements. The dynamic range and the sensitivity were determined for nanoparticle labelling with and without metal enhancement. Nanoparticle concentrations down to the fM range could be detected. The ultimate limit of detection, the identification of individual labels, is demonstrated for the optical readout. Therefore, AFM images of the particles were correlated with the optical signal of individual or clustered particles. We demonstrate that the optical signal allows the identification of single particles.

(Some figures in this article are in colour only in the electronic version)

1. Introduction

In the early 1990s micro-array-based biological chip techniques emerged as a novel approach for molecular detection (Skena *et al* 1998, Skena 2003). These technologies are based on affinity assays in highly parallelized form. High throughput systems are realized with miniaturized molecule libraries in lateral arrangement on planar surfaces, which were used for both synthesis and detection. The selection of the assay is usually based on the choice probe molecules and the possibility of optical detection. Standard labelling is fluorescence-based. Nanoparticle labelling of DNA molecules (Mirkin *et al* 1996, Alivisatos *et al* 1996) pointed to an alternative marker for the detection of hybridization events. This label is compatible with chip techniques (Taton *et al* 2000, Reichert *et al* 2000). There is a variety of detection schemes available: a scanning force microscopic (AFM) characterization of such samples yields exact values for the particle densities by resolving every single nanoparticle (Csáki *et al* 2001). An electrical selection of the

hybridizing assay was realized using microstructured electrode gaps (Park *et al* 2002, Möller *et al* 2001), and a readout system with a computer-controlled measurement unit was described (Urban *et al* 2003). An optical detection of the nanoparticle labelling on transparent biological chips can be carried out with simple instrumentation. The amplification of the signal, by means of special silver enhancement, increases the sensitivity of optical detection, and allows the readout by simple desktop scanners (Taton *et al* 2000).

Here we report a parallel ultramicroscopic and optical characterization of silver-enhanced gold nanoparticle labelling. Surface densities of particles can be related to a given optical absorption. Under certain conditions (regarding surface density and enhancement time), individual nanoparticles are resolvable in the optical contrast. By the correlation of atomic force microscope (AFM) and optical images of the very same particle, the number of particles responsible for an individual optical signal could be clearly identified. This identification was based on the intensity of the optical response from an individual signal.

2. Materials and methods

2.1. The preparation of capture oligonucleotide self assembly monolayer

Glass substrates 4 mm × 25 mm were cut from slides (Roth, Karlsruhe, Germany). The substrates were cleaned by Piranha solution (sulphuric acid and hydrogen peroxide in a mixing ratio of 70% and 30%) and plasma etching. Afterwards, the substrates were incubated in 1% APTES (3-aminopropyltriethoxysilane, Fluka, Buchs, Switzerland) in acetone for 1 h at room temperature. After five washing steps in acetone for 5 min, each substrate was dried at 110 °C for 45 min. A 2 h incubation with 2% 1,4-phenylenediisothiocyanate (PDC, Fluka, Buchs, Switzerland) in 10% pyridine/dimethylformamide (Sigma-Aldrich, Taufkirchen, Germany) was followed by washing steps with methanol and acetone, prior to drying.

Amino-modified capture DNA oligonucleotides (2 mM, H₃N-(CH₂)₅-3'-TCCAGCGG-CGGGTCAGTCAGTCAGTCAGTCAGTCA-5', Jena BioScience, Germany) were dissolved in 100 mM carbonate/bicarbonate buffer, followed by an incubation with the silanized and PDC-modified substrates at 37 °C for 2 h. After DNA immobilization the substrates were washed with ammonia solution (1×) and water (3×), and then dried.

The substrates were marked with a cross using a marker pen to enable identification of the same surface location for parallel optical and AFM imaging.

2.2. The preparation of gold-labelled probes

Gold nanoparticles were functionalized with thiol-modified oligonucleotides. 5-alkylthiolated probe oligonucleotides (3'-GGAACACGATCACTTTAGTAGAGCG5'-(CH₂)₆-SH, Jena BioScience, Germany) were purified using a NAP-10 column (Amersham Pharmacia, Freiburg, Germany). A pre-incubation of oligonucleotides with gold nanoparticle solution (30 nm diameter; Plano/British BioCell, Wetzlar, Germany) in a ratio of 0.33 nM gold and 200 nM oligos for 16 h at room temperature was conducted. In the next step an incubation for 48 h in an adjusted buffer (0.1 M NaCl/10 mM sodium phosphate buffer at pH 7.0) was carried out. The complex was washed several times with buffer. The concentrations were adjusted by centrifugation and subsequent dilutions.

2.3. Sandwich hybridization

In the first hybridization step, the complementary target binds to the immobilized capture oligonucleotide. The solution of 1 μM target (5'-AGGTCGCCGCC(AGTC)₁₆CTTGTC-CTA GTGAAATCATCTCGC-3', Jena BioScience, Germany) in 1 M NaCl/TE buffer was incubated at 72 °C for 20 min and slowly cooled down to 52 °C. After the first hybridization step, excess DNA was removed by washing at room temperature with filtered deionized water.

In the second hybridizing step, the immobilized target was labelled with nanoparticle probes. A nanoparticle concentration of about 0.0001–0.25 OD_{525 nm} (33 fM–83 pM in 0.1 M NaCl/10 mM sodium phosphate buffer at pH 7.0) was utilized in a 20 min incubation at 52 °C, prior to slow cooling to room temperature and final washing steps.

2.4. Signal enhancement

The silver enhancement SEKL 15 (Plano/British BioCell, Wetzlar, Germany), a mixture of initiator and enhancer (in 1:1 per volume), was used for 10 min at room temperature. Afterwards the reaction is blocked by water.

2.5. Microscopical and optical characterization

For the optical characterization of the samples in transmission and reflection mode an *Axiotech* (Carl Zeiss, Jena, Germany) microscope with a *Sensicam* (PCO Computer Optics, Kehlheim, Germany) CCD camera was used. For quantitative evaluation, the software *Scion Image for Windows Beta 4.0.2* (Scion Corporation, Maryland, USA) was applied, utilizing the grey tone values as basis. Absorption measurement was accomplished with a custom-built optical evaluation unit using wavelengths between 575 and 625 nm. A substrate without nanoparticle labelling (control) and air (reference) were used, respectively.

Ultramicroscopical visualization of individual particles was done by scanning force microscopy (AFM, *NanoScope III* with *Dimension 3100*, Digital Instruments, Santa Barbara, CA) in tapping mode on air. Usually a scan size of 4 and 10 μm was imaged and exported as a TIFF-file.

3. Results and discussion

3.1. Nanoparticle assay

The signal in microarray-format nanoparticle assays is represented by the amount of specifically bound particles (often measured as surface density). This is achieved by immobilization of capture molecules (DNA in the case of DNA chips) in an array pattern on a substrate surface (figure 1(a)). In the case of a sandwich-type assay, the target molecule binds to the immobilized complementary capture probe in a specific reaction (hybridization, figure 1(b)). To detect this binding, a second molecule, that holds a label (nanoparticle), binds specifically to the target (probe, figure 1(c)). To allow for easy detection, an enhancement step can be applied, resulting in enlarged particles by the deposition of metal (figure 1(d)).

AFM images of nanoparticles immobilized according to this scheme are shown in figure 1(e) (without enhancement) and figure 1(f) (after enhancement). Such images resolve clearly the individual particles, and can be applied to determine the exact surface density of the studied surface region. Using AFM, the surface density of nanoparticles depending on the concentration of the solution was studied. For concentrations in the nanometre range, surface densities of about 100–200 particles μm⁻² were measured (Csáki *et al* 2001). Now, we investigated lower concentrations, resulting in surface densities below 10 particles μm⁻² (figure 2(a)). For this concentration range, a linear dependency of the surface density on the concentration was found.

However, AFM imaging has several drawbacks. It is very slow (minutes per image), it can only visualize a limited region of about 100 μm² at a time, and it needs equipment not available in standard biological laboratories. So it is not generally applicable for molecular detection.

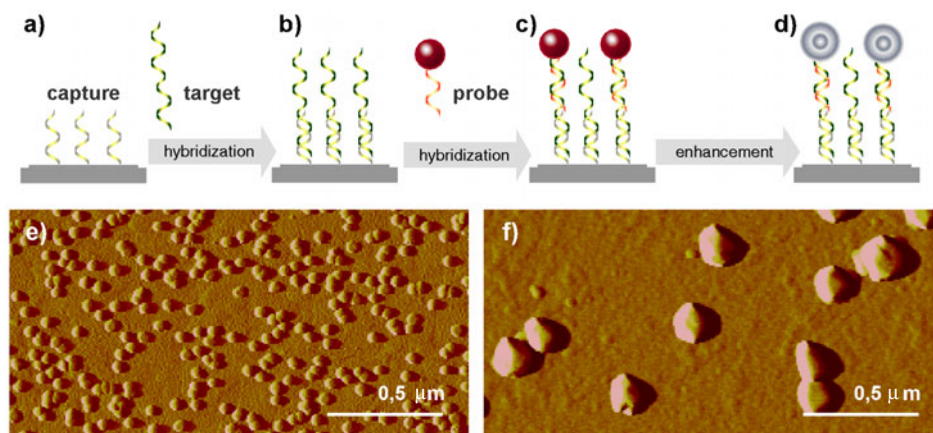


Figure 1. (a)–(d): A schematic representation of a sandwich hybridization assay. Capture: 35 mer amino modified oligonucleotide; target: 100 mer; probe: 25 mer oligonucleotide with 30 nm gold nanoparticle. (e), (f): AFM image of 30 nm gold nanoparticles before (e) and after (f) silver enhancement.

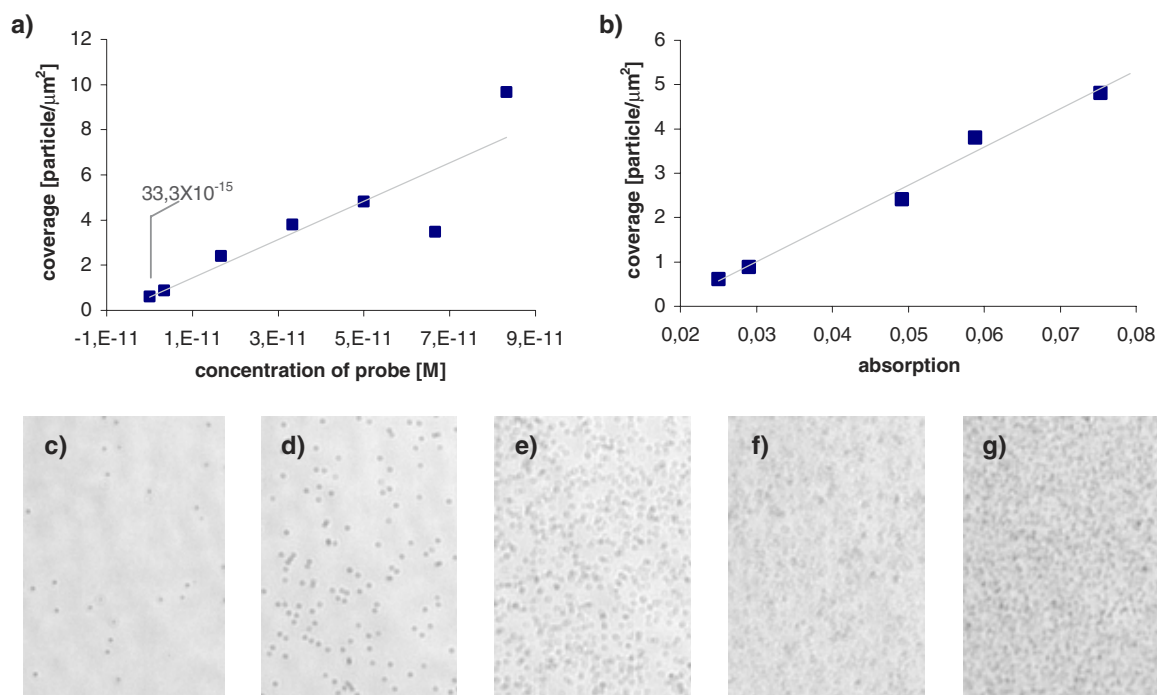


Figure 2. The optical detection of nanoparticle labelling for biochips after silver enhancement: a comparison of the optical and the AFM signal. (a) Particle surface density dependence on concentration; the concentration for the first (left) data point was 33.3 fM. (b) Correlation of particle density and optical signal. (c)–(g) Optical transmission images of the labelled and enhanced samples ($32 \mu\text{m} \times 48 \mu\text{m}$). The concentration increases from left to right.

3.2. Signal enhancement

What are the requirements for today's molecular detection methods? They should be highly sensitive and specific, and at the same time fast and cost-efficient. Parallelization and miniaturization are additional points. Especially the diagnostic field needs techniques that are stable and highly automated, to enable measurements outside dedicated laboratories and nearer the point-of-care. These requirements could be met by straightforward optical methods. They allow a simultaneous readout of whole arrays, and they are established techniques in biological research. The optical readout of 30 nm gold-labelled DNA bound on microstructured DNA spots using a microscope

has been reported (Reichert *et al* 2000). Therefore, both reflection and transmission mode were able to measure a signal related to the surface concentration of nanoparticles. However, for lower densities of particles, the signal of the utilized gold particle was too weak for detection. To increase the signal, an enhancement technique known from electron microscopy (Hacker *et al* 1991) was applied, resulting in silver deposition on the particles. The enhanced particles can be detected by simple means; even a desktop scanner is sufficient (Taton *et al* 2000). The enhancement process can be controlled (e.g. by time), so for example for 20 min standard enhancement with 30 nm initial particle diameter a final diameter of 120 nm can be achieved (Möller, unpublished results). All particles were

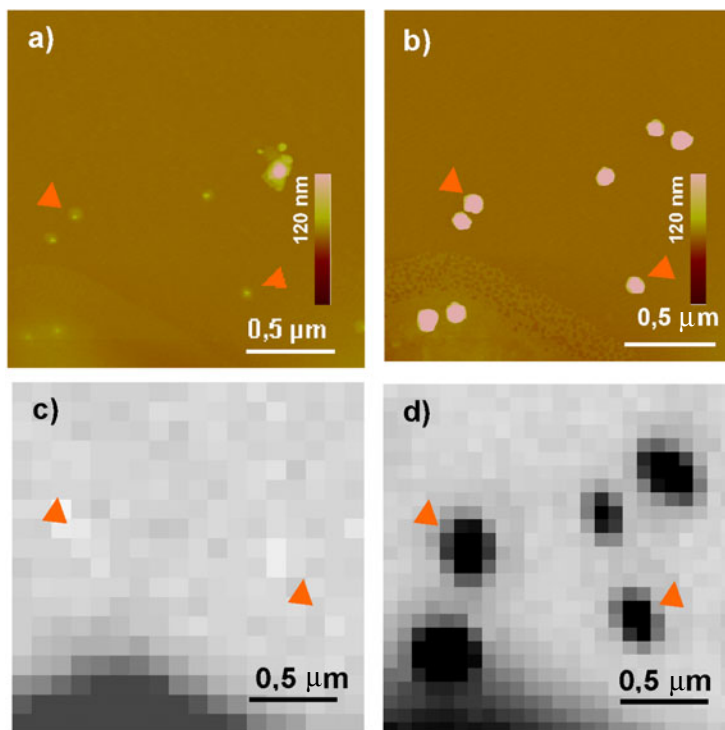


Figure 3. Optical single-particle detection (30 nm nanoparticle probe) before ((a) and (c)) and after ((b) and (d)) silver enhancement. AFM ((a) and (b)) and inverted optical reflection images ((c) and (d)) of selected nanoparticles before (left) and after (right) enhancement.

enlarged in a homogeneous manner. The resulting particle diameter depends only on the original diameter of the particles and the exposition time. The system used, which is based on silver acetate, seems to provide a better homogeneity compared to the silver nitrate system applied e.g. in Park *et al* (2002).

The first demonstrations of silver-enhanced gold nanoparticles for DNA detection in microarray format (Taton *et al* 2000, Alexandre *et al* 2001, Wang *et al* 2003) are promising. Besides the demonstrated stability, sensitivity is an important point on the way to applicability. A broader application needs a better understanding of the signal generation especially in the low signal range to explain measured values and to further increase the sensitivity.

3.3. Optical signal-response curves

We determined the optical absorption of samples with different surface densities of immobilized and metal-enhanced nanoparticles. The same samples were characterized for the determination of surface densities of nanoparticles by AFM (figure 2(a)) and optically. A linear dependency of the optical absorption on the surface density of nanoparticles was observed for these low-density values (figure 2(b)). Such a linear relationship between target concentration, nanoparticle density and optical absorption is the base for a quantification of particle-labelled molecules using AFM or optical methods. Moreover, easy and fast optical methods can be used for a pre-screening of nanoparticle samples in research applications, without the need to scan every sample by time-consuming AFM.

Optical images (transmission) of a concentration series of immobilized and enhanced particles are given in

figures 2(c)–(g). With increasing concentration (from left to right), the substrates appear darker, pointing to a higher absorption. A closer inspection reveals a spotted appearance, especially for lower concentrations. Going down to picomolar concentrations (figures 2(c), (d)), separated spots appear randomly distributed in a rather low density. What is the basis for this effect? A first possibility would be inhomogeneities in surface coverage with nanoparticles, so that particle aggregates or regions with a higher density will show up darker. However, AFM images showed no significant variations in nanoparticle density over the samples on a micrometre scale, thereby rejecting this hypothesis.

3.4. The contribution of a single particle to the signal

Another explanation would be that we see here effects caused by individual enhanced particles. The enhanced particles exhibit diameters of about 100 nm as revealed by AFM, hampering a conventional optical resolution due to these sub-wavelength dimensions. However, because individual nanoparticles are in general detectable by optical means (Schultz *et al* 2000, Yguerabide and Yguerabide 1998), one has to consider this possibility. The density of the spots in the optical image is comparable to the surface density of nanoparticles measured by AFM, supporting the hypothesis.

To confirm this theory, we started experiments to correlate optical images with AFM images of the same surface region, so that ultimately a signal in the optical contrast can be traced back to its origin in the AFM visualization. At first, the influence of the surface density of immobilized nanoparticles had to be considered. The identification of individual nanoparticles from ultramicroscopic (SEM or AFM) images of enhanced

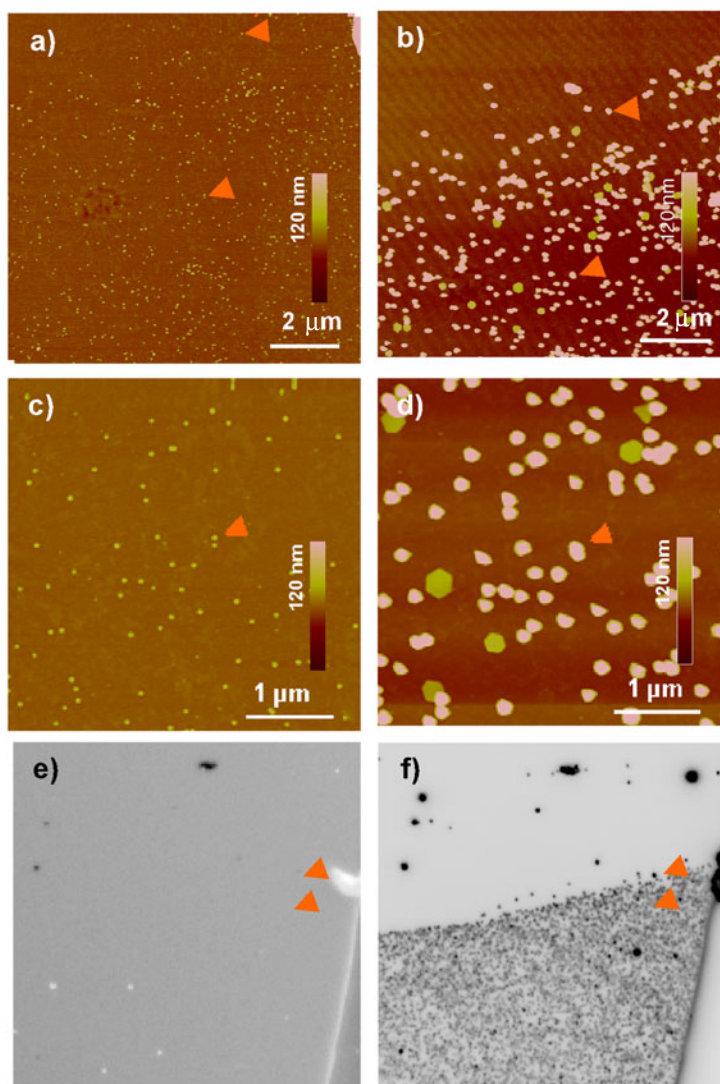


Figure 4. The detection of specifically bound DNA-conjugated nanoparticles (30 nm diameter). AFM ((a)–(d)) and inverted dark field images ((e) and (f)) of selected nanoparticles before (left) and after (right) enhancement. ((e) and (f): 50 μm × 50 μm).

samples is seriously hampered in the case of high density due to the resulting continuous metal layer that is covering the surface (Möller *et al* 2001). Also in the optical contrast, high-density samples are not easily resolvable (figures 2(f), (g)), so that no correlation between optical and topographic signal can be made. Therefore, samples with a low surface density of immobilized nanoparticles were prepared by unspecific adsorption. These samples were imaged before and after silver enhancement by AFM and optical microscopy (figure 3). Care was taken to image the very same regions in all cases. Therefore, pen marks in the vicinity of the region of interest were applied, which were used for alignment of the sample. These marks appear in some images as brighter areas in AFM (e.g. figures 3(a), (b) bottom left) or darker in the optical contrast (e.g., figures 3(c), (d) bottom left).

The 30 nm nanoparticles are detected by AFM (figure 3(a); the curved area on the bottom of the picture is the pen mark). In the respective optical image of this field no nanoparticles are visible, only some artefacts in the reflection mode (figure 3(c)). After enhancement (right), the images changes:

the topographic image (b) visualizes the enhanced particles as rather round structures with increased height and diameter compared to the AFM image before enhancement. These enlarged particles change the optical image significantly: while only the pen mark is visible before enhancement (c) many dark features become visible afterwards (d). These structures represent the individual metal-enhanced beads, as one can confirm by comparing the AFM image (b) to the optical image (d) of the same location.

Another set of experiments was conducted using nanoparticle-labelled DNA specifically bound to DNA-modified surfaces. This set-up represents the typical microarray arrangement. AFM images of 30 nm nanoparticles before enhancement are shown in figures 4(a) (overview) and (c). The optical image of this sample before enhancement shows hardly any contrast (figure 4(e)). However, the metal enhancement procedure changes the image significantly: the enhanced particles appear much brighter (indicating an increase in height) and broader compared to the particle imaged before using the same lateral and height scale (figures 4(b), (d)). In

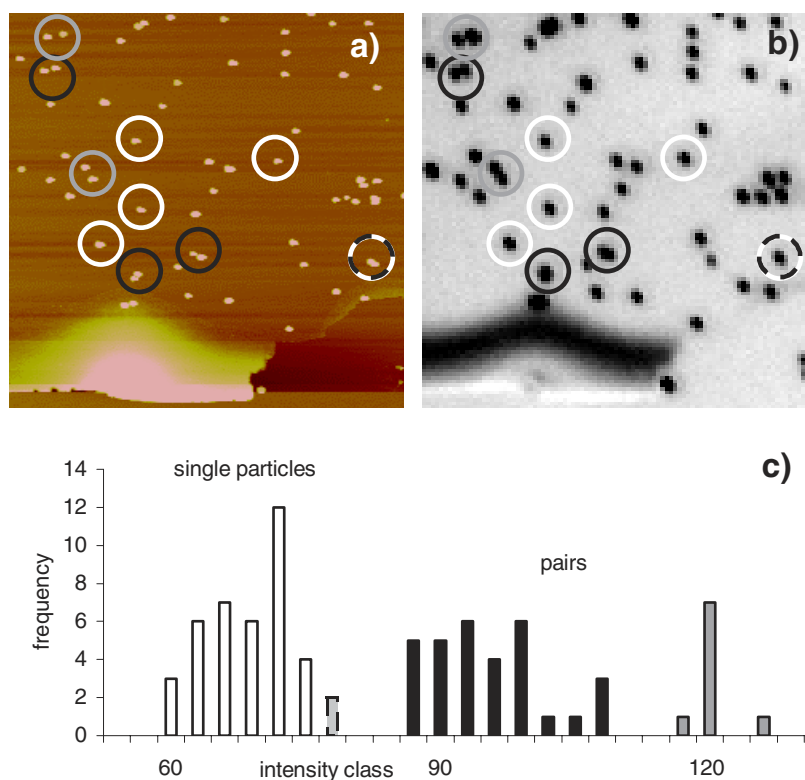


Figure 5. The classification of the optical signal (integrated intensity) of individual particles or pairs of adjacent particles. White: single particles; black: pairs; grey: pairs with larger distance; dashed: nanoparticle pairs with minimal distance. (a) AFM image, (b) optical image ($15 \mu\text{m} \times 15 \mu\text{m}$) of the same region as (a) and (c) the histogram shows the classification of samples according to their intensities.

the inverted optical image, spots become visible, surrounded by areas without particles. The empty areas are due to pen marks. Some particles are labelled by arrowheads for better tracking through the different visualization methods as well as treatments. The upper arrowhead marks an individual particle (figure 4(a)); the lower one points to a pair (zoom in figure 4(c)). Because the centre-to-centre distance of this pair of 30 nm particles is about 90 nm, the space between the particles is originally about 60 nm and therefore comparable to the effect of enhancement (approximately 30 nm growth on each side according to height measurements before and after enhancement). So the enhancement results in fusion of the two separated particles into one structure (arrowhead in figure 4(d)). This process leads to a reduction in feature number, and it could hamper the quantification down to the single particle level. To overcome this limitation, an identification of such events is required.

3.5. The correlation of optical and AFM signal of individual particles

The correlation of the optical signal after enhancement with the AFM image taken before enhancement is needed. Therefore, the optical signal of enhanced particles was characterized using the integral intensity, and compared with the AFM information about the particle number involved in one signal (figure 5). Pairs or individual nanoparticles were identified in the AFM image before enhancement (figure 5(a)), and their optical signal after enhancement (figure 5(b)) was measured and plotted (figure 5(c)). In the intensity plot, one can clearly differentiate between the individual particles (with intensity

values between 60 and 80) and clusters of several particles (with intensities above 90). The intensities of the clusters can be divided into two subpopulations: below and above 110. The class below 110 is caused by pairs of particles with a centre-to-centre distance of about 300 nm; the other population exhibits distances in the range of 600 nm.

In the optical image, particle pairs in different states regarding their shapes can be distinguished. When the interparticle distance becomes smaller, the originally separated two particles touch each other in the optical image, resulting in an '8'-shaped outline. For even smaller distances, this outline shifts to a more elliptical shape. This distance-related shape change can be monitored using the respective AFM images. The AFM images also allow us to exactly define the optical resolution of the system, because the distance of pairs just separated in the optical image can be measured with nanometre resolution. Good examples are the two circled pairs in the upper left corner of the images in figures 5(a), (b). The upper one is just separated in the optical contrast, the other one is still in a connected state. AFM measurements yield distances between the silver-enhanced particles of 440 (upper) and 300 (lower) nm, respectively. So a distance of 440 nm is resolvable, but not 300 nm. This points to an optical resolution of the applied system of about 400 nm.

What parameter causes the apparent two classes in the intensity distribution of nanoparticle pairs? One could speculate that in the rather '8'-shaped outline of two adjacent particles, each particle contributes more to the signal than in the case of stronger overlap with the resulting elliptical shape. Maybe the cleft developing between the particles at increased

distances cannot be resolved in the beginning, so that this area contributes an additional offset to the signal. Further experiments will show if this effect could be responsible for the apparent two classes in the intensity distribution.

4. Summary

The optical signal from silver-enhanced DNA-conjugated nanoparticles was studied after immobilization on glass substrates. A correlation was demonstrated between the surface density of nanoparticles and the signal in optical transmission that allows for a quantification of the nanoparticle coverage using only the optical signal. This association can be applied to deduce the number of immobilized particles by optical means, an interesting approach for both DNA chip detection and the growing application of nanoparticle-modified surfaces in nanotechnology. On the other hand, the results explain the contrast generation for optical nanoparticle readout as a novel detection method for DNA chips and for single molecule techniques. For lower surface densities, the optical signal allows the resolution of individual spots. It is demonstrated that these spots can be classified based on their intensity, and that this classification allows for the identification of single particles.

Acknowledgments

We would like to acknowledge J M Köhler for his initial contributions to this field in our group; H P Saluz for helpful discussions; K Kandra for assistance with substrate preparation and T Henkel for assistance with the optical detection.

This work was funded by the DFG (Fr 1348/1-4).

References

- Alexandre I, Hamels S, Dufour S, Collet J, Zammatteo N, De Longueville F, Gala J L and Remacle J 2001 Colorimetric silver detection of DNA microarrays *Anal. Biochem.* **295** 1–8

- Alivisatos A P, Johnsson K P, Peng X, Wilson T E, Loweth C J, Bruchez M P Jr and Schultz P G 1996 Organization of 'nanocrystal molecules' using DNA *Nature* **382** 609–11
- Csáki A, Möller R, Straube W, Köhler J M and Fritzsche W 2001 DNA monolayer on gold substrates characterized by nanoparticle labelling and scanning force microscopy *Nucleic Acids Res.* **29** E81
- Hacker G W, Danscher G, Graf A H, Bernatzky G, Schiechl A and Grimelius L 1991 The use of silver acetate autometallography in the detection of catalytic tissue metals and colloidal gold particles bound to macromolecules *Prog. Histochem. Cytochem.* **23** 286–90
- Mirkin C A, Letsinger R L, Mucic R C and Storhoff J J 1996 A DNA-based method for rationally assembling nanoparticles into macroscopic materials *Nature* **382** 607–9
- Möller R, Csáki A, Köhler J M and Fritzsche W 2001 Electrical classification of the concentration of bioconjugated metal colloids after surface adsorption and silver enhancement *Langmuir* **17** 5426–30
- Park S J, Taton T A and Mirkin C A 2002 Array-based electrical detection of DNA with nanoparticle probes *Science* **295** 1503–6
- Reichert J, Csáki A, Köhler J M and Fritzsche W 2000 Chip-based optical detection of DNA hybridization by means of nanobead labelling *Anal. Chem.* **72** 6025–9
- Schena M 2003 *Microarray Analysis* (Hoboken, NJ: Wiley-Liss)
- Schena M, Heller R A, Theriault T P, Konrad K, Lachenmeier E and Davis R W 1998 Microarrays: biotechnology's discovery platform for functional genomics *Trends Biotechnol.* **16** 301–6
- Schultz S, Smith D R, Mock J J and Schultz D A 2000 Single-target molecule detection with nonbleaching multicolor optical immunolabels *Proc. Natl Acad. Sci. USA* **97** 996–1001
- Taton T A, Mirkin C A and Letsinger R L 2000 Scanometric DNA array detection with nanoparticle probes *Science* **289** 1757–60
- Urban M, Möller R and Fritzsche W 2003 A paralleled readout system for an electrical DNA-hybridization assay based on a microstructured electrode array *Rev. Sci. Instrum.* **74** 1077–81
- Wang Y F, Pang D W, Zhang Z L, Zheng H Z, Cao J P and Shen J T 2003 Visual gene diagnosis of HBV and HCV based on nanoparticle probe amplification and silver staining enhancement *J. Med. Virol.* **70** 205–11
- Yguerabide J and Yguerabide E E 1998 Light-scattering submicroscopic particles as highly fluorescent analogs and their use as tracer labels in clinical and biological applications I. Theory *Anal. Biochem.* **262** 137–56